D. Rozumek et alii, Frattura ed Integrità Strutturale, 42 (2017) 23-29; DOI: 10.3221/IGF-ESIS.42.03

Focused on Mechanical Fatigue of Metals

Fatigue crack growth in 2017A-T4 alloy subjected to proportional bending with torsion

D. Rozumek, S. Faszynka
Opole University of Technology
d.rozumek@po.opole.pl, sebastian.faszynka@op.pl

ABSTRACT. The paper presents the results of tests on the fatigue crack growth for a constant moment amplitude under combined bending with torsion in the aluminium alloy AW-2017A-T4. The tests were performed under different values of the load ratio R. Plane specimens with stress concentrators in form of the external one-sided sharp notch were tested. A non-uniform fatigue cracks growth on both lateral surfaces of specimens was observed during experimental tests. Fatigue cracks were developing in the specimens in two stages; quarter-elliptic edge cracks were observed at the beginning, then evolving into through cracks.

KEYWORDS. Fatigue crack growth; Load ratio; Notch; Bending with torsion.

Citation: Rozumek, D., Faszynka, S., Fatigue crack growth in 2017A-T4 alloy subjected to proportional bending with torsion, Frattura ed Integrità Strutturale, 42 (2017) 23-29.

Received: 31.05.2017
Accepted: 07.06.2017
Published: 01.10.2017

INTRODUCTION

Fatigue of materials, especially formation of fatigue cracks and their growth belong to the most important problems of solid mechanics, and they have been intensely investigated for many years [1, 2]. These phenomena are extremely important, because they damage components of machines, and in many cases they cause disasters. Descriptions of fatigue crack growth under bending with torsion of elements with rectangular cross sections are rarely discussed in the literature. Reason behind this is that such elements are less widely used in the industry. In the literature can be found various problems of fatigue crack growth for simple load conditions, such as: tension, torsion or bending [3-6], as well as for complex load conditions, including: tension with torsion [7], bending with torsion [8], and others [9-11]. The paper [12] the authors described propagation of short cracks and fatigue cracks within threshold range on specimens under three-point bending, during which the researchers initiated crack plane at a certain angle towards bending plane. That allowed obtaining combination of normal and shearing stresses in the crack tip. In Ref. [13] presented three-point cyclic bending of specimens with slits for mixed modes I and III in threshold cracking range. While the performed tests of steel specimens domination of mode I was expected. At the initial stage, changes of mode I were observed, next a fluent rotation of the crack front occurred up to the moment of its perpendicular positioning to the specimen side.
The aim of the paper is to describe fatigue cracks growth in specimens with rectangular cross-section made of the AW-2017A-T4 aluminium alloy under bending with torsion.

EXPERIMENTAL PROCEDURE

Material and specimen

Specimens with rectangular cross-section and gross size 8 x 10 mm were used in fatigue tests. The specimens were made of the AW-2017A-T4 aluminium alloy and described in the standard PN-EN 573 of 1997. Mechanical properties of the material are given in Tab. 1. The specimens were made of a extruded bar 16 mm in diameter.

σ_y (MPa)	σ_u (MPa)	E (GPa)	ν
382	480	72	0.32

Table 1: Mechanical properties of the AW-2017A-T4 aluminum alloy.

The specimens had an external, unilateral notch, which was a_0 = 2 mm long and its radius was ρ = 0.2 mm (Fig. 1). The notches in the specimens were cut with a milling cutter and their surfaces were polished on abrasive paper with decreasing gradation. The theoretical stress concentration factor in the specimen under bending K_t = 3.76 was estimated according to Ref. [14].

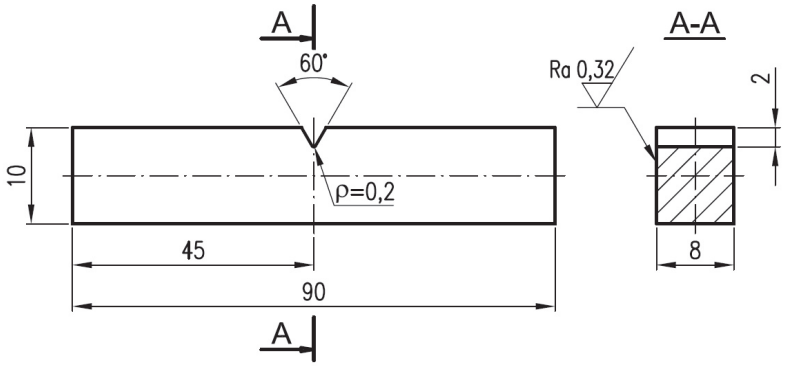

Figure 1: Shape and dimensions of specimen (in mm).

Alloys of aluminium with copper and magnesium, that is duralumin, belong to alloys characterised by supreme strength properties. Elements of such shape are used, among others, in cars (by Renault Co.), trucks and tanks (attaching springs) as torsion bars, and as indirect beams used in drilling for oil and natural gas. Fig. 2 shows a microstructure of the AW-2017A-T4 aluminium alloy. The microstructure heavily dominated by elongated grains of the solid solution α of various sizes, and a width of about 50 μm. Between large elongated grains are also visible cluster very small equiaxed α phase grains in the system band. On a background of solid solution α, there are many precipitation of intermetallic phases, particularly Al_2Cu, as well as Mg_2Si, AlCuMg. Precipitations phase Al_2Cu occur mainly in the chain system on grain boundaries of the solid solution, and their size does not exceed 5 mm [15].

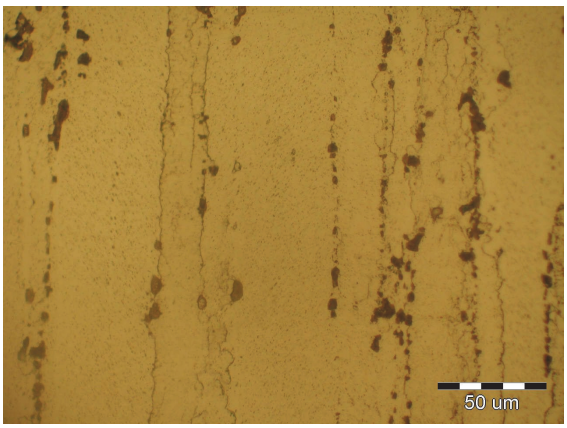

Figure 2: Microstructure of the AW-2017A-T4 aluminum alloy.

Fatigue tests

The test results of fatigue crack growth under proportional bending with torsion were obtained at the laboratory in Department of Mechanics and Machine Design in Opole University of Technology. The tests were performed on the fatigue test stand MZGS – 100 [16, 17], which allows to perform cyclic bending, torsion and synchronous bending with torsion. The tests were conducted under controlled force (in the considered case, the amplitude of bending moment was controlled) with the loading frequency 28.4 Hz. The bending with torsion moment was generated by force on the arm 0.2 m in length. Fatigue tests were performed in the low cycle fatigue (LCF) and high cycle fatigue regime (HCF). Unilaterally restrained specimens were performed with the constant amplitude of moments M_a = 7.92 N·m and load ratio R = M_{min} / M_{max} = - 1, 0. The shear stress at the specimen coming from bending takes very small values, below 3% of the maximum applied bending stress and it is neglected in further considerations. In Fig. 3 M(t) is the ratio of torsion moment to bending moment was $M_T(t) / M_B(t) = \tan\alpha = 1$. Proportional bending with torsion were obtained by rotation of the head by angle α = 45° (see Fig. 3). Pure bending takes place when the α angle is 0°, and for the α angle 90° we have torsion.

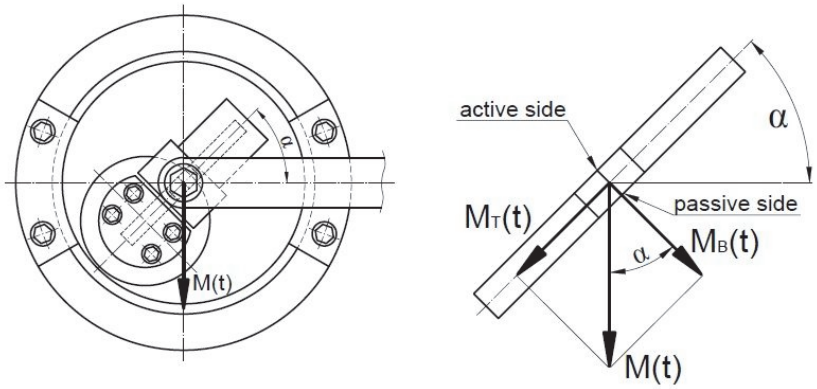

Figure 3: Loading of the specimen under proportional bending with torsion.

Fatigue crack growth on the specimen lateral surfaces – "a" (active side) and "a*" (passive side) and upper surface "c" (Fig. 4) was observed with the portable optical microscope with magnification of 20 times. The fatigue crack increments were measured with the micrometer of accuracy up to 0.01 mm with the corresponding number of loading cycles N.

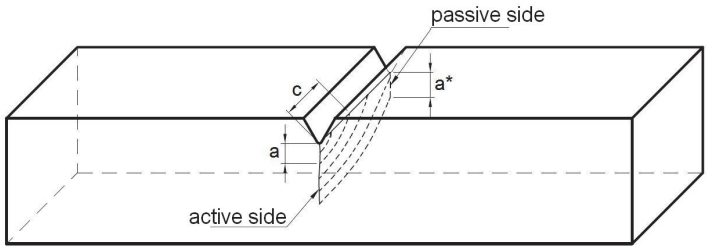

Figure 4: Crack growth under proportional bending with torsion.

EXPERIMENTAL RESULTS AND DISCUSSION

A non-uniform fatigue cracks growth on both lateral surfaces of specimens was observed during experimental tests. Fatigue cracks were developing in the specimens in two stages; quarter-elliptic edge cracks were observed first, then evolving into through cracks. Experimental test results for proportional bending with torsion are shown as diagrams of crack lengths: a = f (c) (Fig. 5a), a = f (a*) (Fig. 5b) and a = f (N) (Fig. 6). Growth period for quarter-elliptic edge cracks at load ratio R = -1 was ca. 27% of specimen lifetime, whereas for through cracks its value reached approximately 73%. For load ratio R = 0 growth period for quarter-elliptic edge cracks was ca. 18% of specimen lifetime, whereas for through cracks it reached approximately 82%. From graphs fatigue cracks growth shown in Fig. 5a allowed observing that for load ratio R = -1 the relationship between lengths of cracks a/c had higher values than for ratio R = 0. For example, Fig. 5a shows that for ratio R = -1 and c = 7.20 mm (crack depth in specimen upper surface) the

relationship between lengths of cracks is: a/c = 0.274, whereas for ratio R = 0 and c = 7.20 mm this relationship is: a/c = 0.174. The results of crack length measurements a = f (c) show higher curvatures for ratio R = -1 than for R = 0. Fig. 5b presents experimental test results performed for the same specimen as in Fig. 5a, but for further through crack growth. Figs. 5a and 5b demonstrate in diagrams non-uniform fatigue cracks growth on both specimen active side and passive side. Higher crack growth values were measured for active side than passive side. Test results (Fig. 5b) allowed observing that for load ratio R = -1 and crack length a = 7.10 mm, the relationship a/a* = 1.203 has higher values than for the ratio R = 0, where a/a* = 1.092. Whereas, for R = -1 and a* = 0.15 mm, the relationship a/a* = 14.333 also has higher values than for the ratio R = 0, which is a/a* = 10.133. We may also observe that for a* = 0.15 mm the relationship a/a* is approximately twelve times (R = -1) and nine times higher (R = 0) than for a = 7.10 mm. Moreover, experimental test results shown in Fig. 5b allow observing that during the final cracking stage, the lengths of cracks on the sides active and passive, for R = 0, are close to each other, and for R = - 1 the difference between these lengths is higher.

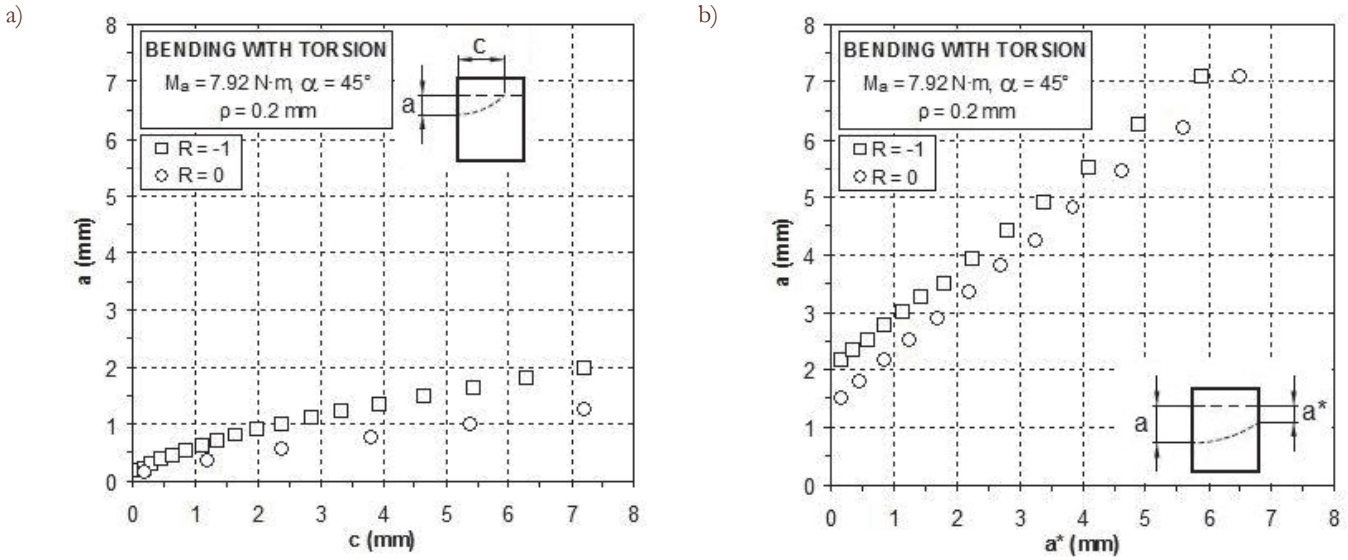

Figure 5: Fatigue crack length under bending with torsion for: a) cracks edge quarter-elliptic, b) through cracks on both specimen sides: active and passive.

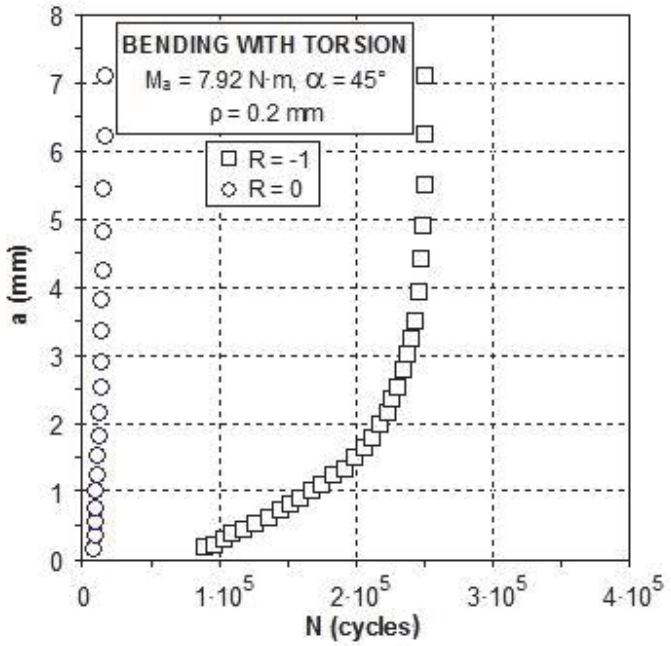

Figure 6: Fatigue crack length „a" versus number of cycles N (active side specimen).

Fig. 6 shows experimental test results in the form of diagrams the lengths of fatigue cracks "a" in function of the number of cycles N. During the test analysis it has been observed that fatigue life increases more than 14 times, changing ratio value from R = 0 to R = -1. For specimens subjected to oscillatory loads (R = -1), cracking initiation commenced after 90000 cycles (fatigue failure was formed after 251000 cycles), whereas for R = 0 cracking initiation took place already after 9000 cycles (failure was formed after 17500 cycles). The tests were performed for three specimens at each load level.
Fig. 7 presents experimental test results in the form of diagrams showing fatigue crack growth rate da/dN (dc/dN) in function of changes equivalent stress intensity factor range ΔK_{eq}. The increase in fatigue crack growth rate da/dN applies to specimen length (active side), whereas dc/dN concerns specimen depth. Test results for fatigue crack growth rate in function of equivalent stress intensity factor range were described using Paris equation [18]

$$\frac{da}{dN}=\frac{dc}{dN}=C\left(\Delta K_{eq}\right)^{m} \tag{1}$$

a)

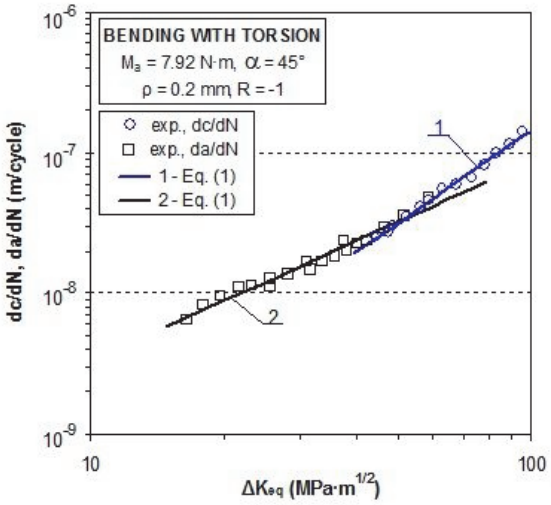

b)

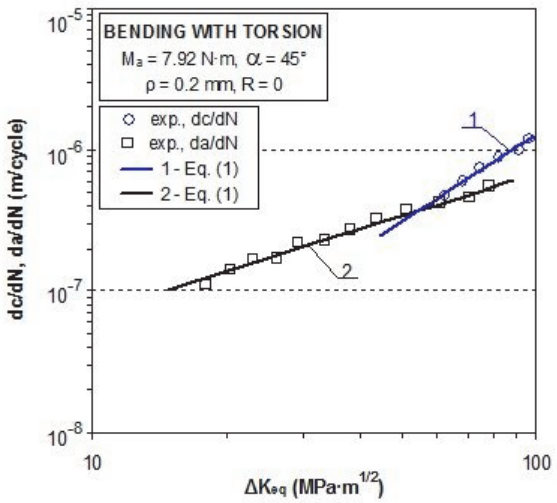

Figure 7: Comparison of the test results with calculations according to Eq. (1) for specimens under bending with torsion: a) R = -1, b) R = 0.

In case of proportional loads (bending with torsion), equivalent stress intensity factor range ΔK_{eq} for mixed cracking mode was computed using the following formula

$$\Delta K_{eq}=\sqrt{\Delta K_{I}^{2}+2.64\Delta K_{III}^{2}} \tag{2}$$

A changes range of the stress intensity factor ΔK_I for bending (mode I) and ΔK_{III} for torsion (mode III) was calculated from [13]

$$\Delta K_{I}=Y_{I}\Delta\sigma\cos^{2}\alpha\sqrt{\pi\left(a_{0}+a\right)} \tag{3}$$

$$\Delta K_{III}=Y_{III}\Delta\sigma\sin\alpha\cos\alpha\sqrt{\pi\left(a_{0}+a\right)} \tag{4}$$

where $\Delta\sigma$ – range of nominal stresses under bending and torsion.
The correction coefficients Y_I for bending [19] and Y_{III} for torsion [20] occurring in Eqs. (3) and (4) take the following forms

$$Y_{I}=5/\sqrt{20-13\left(\left(a_{0}+a\right)/h\right)-7\left(\left(a_{0}+a\right)/h\right)^{2}} \tag{5}$$

$$Y_{III} = \sqrt{\left(2h/\left(a_0 + a\right)\right)\tan\left(\pi\left(a_0 + a\right)/2h\right)} \quad (6)$$

where h – height of the specimen.

Fig. 7 allows observing that change of ratio R = -1 to R = 0 results in increasing fatigue crack growth rate da/dN (dc/dN). For instance, in case of constant value of stress intensity factor range ΔK_{eq} = 33 MPa·m$^{1/2}$, crack growth rate along the length increases from da/dN = 1.69·10^{-8} m/cycle (R = -1) to da/dN = 2.30·10^{-7} m/cycle (R = 0). The increase is more than 13 times. Whereas, for other example of constant parameter ΔK_{eq} = 68 MPa·m$^{1/2}$, crack growth rate along the depth increases from dc/dN = 5.93·10^{-8} m/cycle (R = -1) to dc/dN = 6.06·10^{-7} m/cycle (R = 0). The increase exceeds 10 times.

Coefficients C and m occurring in formula (1), determined on the basis of experimental tests, were computed using the least squares method. They are shown in Tab. 2, which also specifies correlation coefficients r. Test results for proportional bending with torsion are burdened with relative error not exceeding 13% at significance level α = 0.05. In all cases, correlation coefficients r, have values close to 1, which proves significant correlation of experimental test results and the approved Eq. (1). Moreover, Tab. 2 allows finding that coefficients C and exponents m for R = -1 and R = 0 (da/dN and dc/dN) have different values. Differences in the values of coefficients C and m prove that load ratio R affects shift C and inclination m of the curve.

Figures	curves	R	C, m(MPa·m$^{1/2}$)$^{-m}$/cycle	m	r
7a	1 (depth)	-1	5.784·10^{-12}	2.201	0.995
7a	2 (length)	-1	1.299·10^{-10}	1.409	0.985
7b	1 (depth)	0	1.131·10^{-10}	2.026	0.991
7b	2 (length)	0	7.183·10^{-9}	0.988	0.993

Table 2: Coefficients C and m of Eq. (1) and correlation coefficients r for the curves shown in Fig. 7.

CONCLUSIONS

The following conclusions have been made on the basis of the obtained results fatigue cracks growth:

- Under proportional bending with torsion was observed two stage fatigue cracks growth, quarter-elliptic edge cracks, which then passes through the crack.
- It was noticed that the difference in lengths of cracks on both specimen sides is higher for load ratio R = -1 than for R = 0.
- The fatigue crack growth rate is higher for dc/dN compared with da/dN under the same value ΔK_{eq}.
- It has been confirmed that the change of ratio R = 0 to R = -1 results in fatigue life increase exceeding 14 times, while at the same time crack growth rate drops by more than 10 times.

REFERENCES

[1] Kocańda, S., Fatigue failure of metals, WNT, Warszawa, (1985).
[2] Pyrzanowski, P., Estimation and consequences of the crack thickness parameter in the assessment of crack growth behaviour of "squat" type cracks in the rail–wheel contact zone, Engineering Fracture Mechanics, 74 (2007) 2574-2584.
[3] Rozumek, D., Marciniak, Z., Fatigue properties of notched specimens made of FeP04 steel. Materials Science, 47(4) (2012) 462-469.
[4] Gadomski, J., Pyrzanowski, P., Experimental investigation of fatigue destruction of CFRP using the electrical resistance change method, Measurement, 87 (2016) 236-245.
[5] Martins, R. F., Ferreira, L., Reis, L., Chambel, P., Fatigue crack growth under cyclic torsional loading, Theoretical and Applied Fracture Mechanics, 85 (2016) 56-66.

[6] Rozumek, D., Bański, R., Crack growth rate under cyclic bending in the explosively welded steel/titanium bimetals, Materials & Design, 38 (2012) 139-146.
[7] Gladskyi, M., Fatemi, A., Notched fatigue behavior including load sequence effects under axial and torsional loadings, International Journal Fracture, 55 (2013) 43-53.
[8] Gasiak, G., Robak, G., Simulation of fatigue life of constructional steels within the mixed modes I and III loading, Fatigue & Fracture of Engineering Materials & Structures, 34 (2011) 389-402.
[9] Carpinteri, A., Brighenti, R., Part-through cracks in round bars under cyclic combined axial and bending loading, International Journal of Fatigue 18, (1996) 33-39.
[10] Spagnoli, A., Carpinteri, A., Ferretti, D., Vantadori, S., An experimental investigation on the quasi-brittle fracture of marble rocks, Fatigue & Fracture of Eng. Mat. & Structures, 39 (2011) 389-402.
[11] Rozumek, D., Macha, E., J-integral in the description of fatigue crack growth rate induced by different ratios of torsion to bending loading in AlCu4Mg1, Materialwissenschaft und Werkstofftechnik, 40(10) (2009) 743-749.
[12] Yates, J. R., Miller, K. J., Mixed mode (I+III) fatigue thresholds in a forging steel, Fatigue & Fracture of Eng. Mat. & Structures, 12 (1989) 259-270.
[13] Pook, L.P., The fatigue crack direction and threshold behaviour of mild steel under mixed mode I and III loading, Int. J. Fatigue, 7 (1985) 21-30.
[14] Thum, A., Petersen, C., Swenson, O., Verformung, Spannung und Kerbwirkung. VDI, Düesseldorf, (1960).
[15] Rozumek, D., Marciniak, Z., Fatigue crack growth in AlCu4Mg1 under nonproportional bending with torsion loading, Materials Science, 46 (2011) 685-694.
[16] Lewandowski, J., Rozumek, D., Cracks growth in S355 steel under cyclic bending with fillet welded joint, Theoretical and Applied Fracture Mechanics, 86 (2016) 342-350.
[17] Rozumek, D., Marciniak, Z., Control system of the fatigue stand for material tests under combined bending with torsion loading and experimental results, Mechanical Systems and Signal Processing, 22(6) (2008) 1289-1296.
[18] Paris, P. C., Erdogan, F., A critical analysis of crack propagations laws, Journal of Basic Engineering, Trans, American Society of Mechanical Engineers, 85 (1963) 528-534.
[19] Picard, A. C., The application of 3-dimensional finite element methods to fracture mechanics and fatigue life prediction, Chameleon Press LTD, London, (1986).
[20] Chell, G.G., Girvan, E., An Experimental Technique for Fast Fracture Testing in Mixed Mode, Int. J. Fracture, 14 (1978) 81-84.

NOMENCLATURE

a_0	notch length
a	active crack length
a*	passive crack length
c	crack depth
da/dN	fatigue crack growth rate along the length
dc/dN	fatigue crack growth rate along the depth
E	Young's modulus
K_t	theoretical stress concentration factor
M_a	amplitude of moments
N	number of cycles crack growth
R	load ratio
t	time
α	means arctan (M_T/M_B) of the ratio of the torsional moment to the bending moment
ν	Poisson's ratio
σ_u	ultimate tensile stress
σ_y	yield stress
ΔK_{eq}	equivalent stress intensity factor range